International Journal of Mass Spectrometry 330–332 (2012) 118–123

Contents lists available at SciVerse ScienceDirect

International Journal of Mass Spectrometry

journal homepage: www.elsevier.com/locate/ijms

Gas-phase infrared spectrum of the anionic GFP-chromophore

Mitra Almasian[a,b], Josipa Grzetic[a], Giel Berden[a], Bert Bakker[b], Wybren Jan Buma[b,*], Jos Oomens[a,b,c,**]

[a] FOM Institute for Plasma Physics Rijnhuizen, Edisonbaan 14, 3439MN Nieuwegein, The Netherlands
[b] Van 't Hoff Institute for Molecular Sciences, University of Amsterdam, Science Park 904, 1098XH Amsterdam, The Netherlands
[c] Radboud University Nijmegen, Institute for Molecules and Materials, Heyendaalseweg 135, 6525AJ Nijmegen, The Netherlands

ARTICLE INFO

Article history:
Received 29 June 2012
Received in revised form 8 August 2012
Accepted 8 August 2012
Available online 20 August 2012

Dedicated to Peter B. Armentrout on the occasion of his 60th birthday and in recognition of his seminal contributions to ion chemistry.

Keywords:
Green fluorescent protein
Chromophore
Infrared
Ion spectroscopy
Anion

ABSTRACT

The gas-phase IR spectrum of the anionic chromophore of the green fluorescent protein (*p*-hydroxy-benzylidene-2,3-dimethylimidazolidinone, HBDI) is recorded in the 800–1800 cm^{-1} frequency range using the free electron laser FELIX in combination with an electrospray ionization (ESI) Fourier transform ion cyclotron resonance (FTICR) mass spectrometer. The spectrum is substantially different from IR spectra of the anion recorded previously in solution, which were found to be difficult to interpret on the basis of electronic structure calculations involving the polarisable continuum model (PCM) method. In contrast, the IR spectrum of the isolated anion recorded here matches favourably with its DFT calculated counterpart if diffuse functions are included in the basis set. IR photo-fragmentation of the HBDI anion proceeds *via* loss of a methyl radical ($CH_3^{\bullet}$) resulting in an odd-electron product anion. The IR spectrum of this radical anion photoproduct is also recorded, which indicates that the radical site resides on the imidazolinone nitrogen atom where the methyl group is detached.

1. Introduction

The discovery of the green fluorescent protein (GFP) [1] in the jellyfish *Aequorea victoria* has revolutionized imaging methods in molecular cell biology and has been key to the study of energy transfer in proteins by application of Förster resonance energy transfer (FRET). The fluorescent chromophore of GFP, *p*-hydroxy-benzylidene-2,3-dimethylimidazolidinone (HBDI), is formed post-translationally from the Ser65-Tyr66-Gly67 sequence of the protein [2]. X-ray crystallographic studies show that the chromophore is embedded inside a beta-barrel structure in the core of the 238-residue protein and acts as a photoacid: upon photo-excitation the chromophore transfers a proton to the protein matrix adopting its anionic phenolate form (see Scheme 1), which is responsible for the fluorescent properties of the chromophore [3–5]. Inside the protein pocket, the chromophore is subject to multiple interactions with the protein matrix, which sensitively determine the photochemical properties of the chromophore. Protein engineering has hence resulted in a large variety of GFP mutants with improved fluorescent properties [6,7]. Importantly, variants have been developed in which HBDI can be reversibly switched between the non-fluorescent *trans*- and the active *cis*-conformation [8,9]. In recent variants the wavelength for photo-switching the chromophore between *cis*- and *trans*-conformations is different from that for photo-excitation of the anionic chromophore, providing an independent optical "on/off" switch for the fluorescence activity of the chromophore [10].

In addition to the photochemical properties of the protein, numerous studies have addressed the fluorescent properties of isolated HBDI. In the unique microenvironment of the protein pocket, fluorescence of the chromophore is favoured over non-radiative relaxation by both steric hindrance and electronic effects [11]. In contrast to the fluorescence spectrum of the protein, the emission spectrum of the isolated anionic HBDI chromophore in solution is rather broad and structureless, suggesting that the chromophore experiences a significantly larger conformational freedom when it is removed from the protein environment [12]. Moreover, the fluorescence intensity is partly quenched at room temperature but recovers at 77 K [12,13], suggesting that deactivation pathways become allowed by thermal motion. It has been suggested that excited state isomerisation directly influences the fluorescence quantum yield [14]. In order to study the intrinsic properties of HBDI, that is, in the absence of interactions with the solvent,

* Corresponding author.
** Corresponding author at: Radboud University Nijmegen, Institute for Molecules and Materials, Heyendaalseweg 135, 6525AJ Nijmegen, The Netherlands.
Tel.: +31 24 3653935.
E-mail addresses: w.j.buma@uva.nl (W.J. Buma), joso@rijnhuizen.nl (J. Oomens).

1387-3806/$ – see front matter
http://dx.doi.org/10.1016/j.ijms.2012.08.017

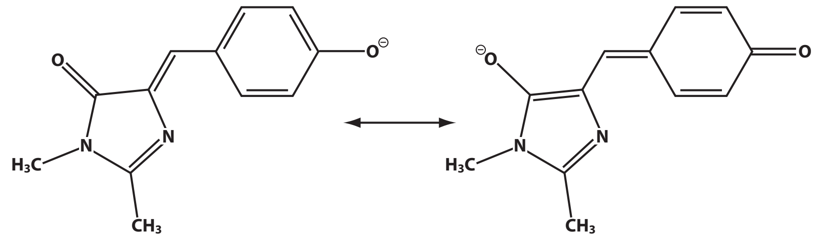

Scheme 1. Deprotonated 4-hydroxybenzylidene-1,2-dimethylimidazolinone (HBDI) as model for the GFP chromophore. The two resonance forms of the anion efficiently delocalize the charge over the entire molecule.

various investigations have recently addressed the properties of the gas-phase anion using a combination of ion-trapping and laser spectroscopy methods [13,15–19]. Since the fluorescence quantum yield was found to be negligible in the gas phase as well [13,19], excitation spectra were obtained in these studies by monitoring dissociation or photodetachment from the gas-phase anions. The main absorption band of anionic HBDI in solution exhibits a substantial blue-shift as compared with the absorption maximum of the chromophore inside the protein [15,16], while the absorption maximum of the gas-phase HBDI anion at 479 nm agrees well with that of the wild type protein at 480 nm [15,16]. This suggests that the gas phase is a reasonable mimic for the environment inside the protein pocket, which is probably the result of a number of crucial but counteracting contributions [20].

The charge state and conformational structure are thus important parameters that determine the fluorescent properties of the chromophore. While the charge state of the chromophore in the protein can be inferred from the optical absorption bands at 395 nm for neutral HBDI and 480 nm for anionic HBDI, vibrational spectra of the protein chromophore provide more accurate molecular structure information. Hence, various solution-phase studies of the vibrational spectra of HBDI in its protonated, deprotonated and neutral form have been reported [21–24]. Computational modelling of the infrared and Raman spectra used the polarization continuum model (PCM) to account for the effects of solvent interactions on the vibrational spectra [23]. While the computed spectra accurately reproduced the vibrational spectra of neutral and protonated HBDI, the agreement with the anionic chromophore was markedly poorer. Moreover, this study revealed that inclusion of solvent effects using the PCM method has little effect on the computed spectra of neutral and protonated systems. The opposite is true for the computed spectrum of the anion, which alters substantially upon going from the gas phase to the solution phase. This is possibly due to inadequacies of the PCM method to handle, in particular, electronically more diffuse systems, such as the conjugated HBDI anion under study here. In addition, experimental spectra were recorded in a solution that inevitably contained counterions; the extent to which these counterions interact with the HBDI anion, whether this influences the IR absorption spectrum and whether such effects are different for positive and negative ions is generally not known, nor is it taken into account in the calculations.

Here we present the first experimental IR spectrum of the HBDI anion in the gas phase, *i.e.*, devoid of any environmental effects, using a combination of tandem mass spectrometry and a widely tunable infrared free electron laser. The spectrum is compared to the solution-phase spectra reported previously and to DFT calculated spectra.

2. Experimental

IR spectra are recorded by infrared multiple-photon dissociation (IRMPD) of the ions using a Fourier transform ion cyclotron resonance mass spectrometer (FTICR-MS) coupled to the beamline of the infrared free electron laser FELIX, which provides intense, wavelength-tunable IR radiation. The anions are produced by electrospray ionization (ESI, Waters Z-Spray) from a 1 mM solution of HBDI in water/methanol with about 1 mM NaOH added to enhance deprotonation. The anions are sampled through a cone and a skimmer and then accumulated for approximately 5 s in a linear hexapole trap. The ions are subsequently pulse-extracted from the trap and injected into the ICR cell *via* a quadrupole deflector and a 1 m long rf octopole ion guide. The *m/z* 215 anion is SWIFT-isolated [25] and irradiated with the IR beam for about 3 s. A mass spectrum is recorded from which the intensity of the parent ion peak and the IR induced fragment peaks are extracted. This procedure is repeated while the wavelength of FELIX is scanned between 800 and 1800 cm^{-1} in steps of approximately 5 cm^{-1}. An IR spectrum is reconstructed by plotting the fragment ion yield ($\Sigma I_{frag}/[I_{par} + \Sigma I_{frag}]$) as a function of wavelength. The laser bandwidth amounts to about 0.5% of the central frequency. Observed linewidths may thus be slightly different at the low- and high-frequency ends of the spectrum. Typical pulse energies employed are on the order of 50 mJ.

The experimental spectra are compared with theoretical vibrational spectra obtained from quantum-chemical calculations on the anion at the density functional theory (DFT) level. Geometry optimizations and harmonic vibrational frequency calculations are performed with Gaussian03 using the B3LYP functional and various basis sets including and excluding diffuse functions. Calculations modelling the spectrum in solution make use of the polarisable continuum model (PCM) taking water as a solvent and using the RADII = UAHF keyword. Calculated harmonic frequencies are scaled with a factor appropriate for the functional and basis set used as advised by Radom and coworkers [26]; *i.e.*, 0.9627, 0.9648 and 0.9648 for the 6-31G**, 6-31+G** and 6-31++G** basis sets, respectively. For comparison with the experimental data, calculated stick spectra are convoluted with a Gaussian band profile with a fwhm bandwidth of 20 cm^{-1}.

3. Results and discussion

3.1. The HBDI anion at m/z 215

Upon resonant IR irradiation, the HBDI parent anion at *m/z* 215 dissociates, forming a product anion at *m/z* 200. This dissociation presumably occurs by loss of a neutral $CH_3^{\bullet}$ radical, which is in agreement with photo-dissociation studies in the UV/vis range of the spectrum [13]. This somewhat uncommon fragmentation into two radical species, violating Mandelbaum's "even-electron rule" [27], and the molecular structure of the fragment is further addressed below where we discuss the IR spectrum that has been recorded for the *m/z* 200 fragment anion.

The IRMPD spectrum of deprotonated HBDI at *m/z* 215 is shown in Fig. 1 along with calculated spectra using the B3LYP functional and basis sets with (6-31+G**, 6-31++G**) and without (6-31G**) diffuse functions. When the calculated spectra are compared, one

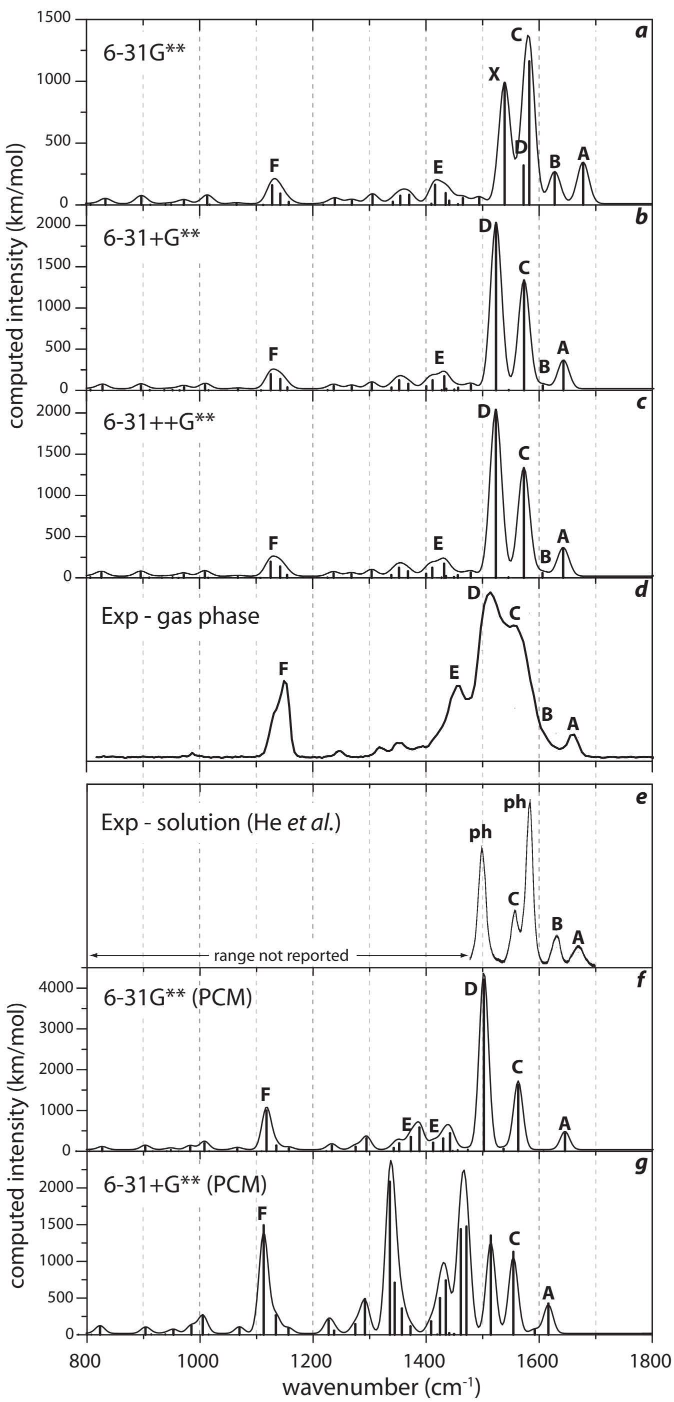

Fig. 1. IRMPD spectrum of anionic HBDI (panel d) compared with calculated spectra using the B3LYP functional and 6-31G**, 6-31+G** and 6-31++G** basis sets (panels a–c). Vibrational bands labelled A through F correlate with entries in Table 1. Panel (e) represents the spectrum of the anion in aqueous solution reported in Ref. [22]. Calculated spectra using the PCM method to model solution-phase spectra are shown in panels (f) and (g).

notices immediately that inclusion of diffuse functions in the basis set, *i.e.*, going from 6-31G** to 6-31+G**, has a substantial influence. This is not surprising as it is well-known that basis sets with diffuse functions substantially improve calculations of the thermochemistry as well as vibrational frequencies for anionic species [28–32]. The variations in the spectrum are particularly noticeable in the region between 1400 and 1700 cm^{-1} where all the strong, diagnostic bands are located. It is further observed that addition of more diffuse functions, *i.e.*, going to the 6-31++G** basis set, does not appreciably change the predicted spectrum any further.

The comparison of computed and experimental spectra in Fig. 1 clearly indicates that inclusion of diffuse functions in the basis set sensitively improves the overall match between experiment and theory. On the basis of the B3LYP/6-31+G** calculation, we thus propose an assignment of experimentally observed absorption bands as listed in Table 1, where letters A through F refer to the corresponding bands in Fig. 1. The weak but well-resolved band at 1660 cm^{-1} at the blue end of the scan range (A) is due to the imidazolinone C═O stretch. Unlike most other bands in the spectrum, the calculations predict a substantially lower frequency (1643 cm^{-1}) for this mode. We attribute this discrepancy to a slightly different scale factor that would be required for this specific mode (see *e.g.*, Refs. [33,34]) and believe its assignment is nonetheless secure given the good overall match of the entire spectrum. The strongest feature in the experimental spectrum clearly consists of two absorption bands centred at approximately 1558 and 1515 cm^{-1} (C and D), which can be assigned to the bands computed at 1574 (imidazolinone C═N stretching) and 1524 cm^{-1} (out-of-phase stretching of the vinyl C═C and phenoxide C—O bonds), respectively. The calculations further show a very weak band at 1606 cm^{-1} (B) associated with the in-phase stretching of the vinyl C═C and phenoxide C—O bonds, which is perhaps just visible as a weak shoulder in the experimental spectrum. The band at 1455 cm^{-1} in the experimental spectrum (E), exhibiting a red wing that extends down to about 1400 cm^{-1}, is assigned to the bands computed between 1400 and 1450 cm^{-1}, which mainly involve the umbrella motions of each of the methyl groups. The apparent blue-shift and intensity enhancement observed in the experimental spectrum may be an artefact of the IRMPD method, which can cause bands on the low-frequency side of strong features to become artificially enhanced [35]. Between 1200 and 1400 cm^{-1} various weak bands are observed, which match approximately with the convolution of the many relatively weak calculated features in this range. The band positions observed in this range are 1355, 1320 and 1250 cm^{-1}; the calculations indicate that they are mainly due to (combined) bending motions of the methyl, vinyl and aromatic hydrogen atoms. The observed spectrum further exhibits a relatively intense and slightly asymmetric feature peaking at 1153 cm^{-1} (F) with a shoulder around 1130 cm^{-1}. This feature matches the two bands calculated at 1143 and 1126 cm^{-1}, which correspond to the in-plane aromatic CH bending mode and a more delocalized hydrogen bending mode, respectively. The calculated spectrum displays various very weak bands further to the red, which are however not clearly observed under the present experimental conditions (note that the tiny feature at 988 cm^{-1} is actually a confirmed absorption). Overall, we find a satisfactory match between the experimental and B3LYP/6-31+G** calculated spectra.

In the lower part of Fig. 1 we show the IR spectrum of the HBDI anion in aqueous solution as reported in Ref. [22]. It should be noticed that in this study only the diagnostic modes between 1500 and 1700 cm^{-1} were reported. Mode assignments were made by isotopic substitution and have been “translated” here into the vibrational mode descriptions used in Table 1. The bands at 1583 and 1499 cm^{-1} indicated in Fig. 1e with ph were referred to as “phenol” modes [22], being mainly phenol CC stretches [24]. Calculated spectra of the anion in solution – generated using the polarisable continuum model (PCM), the 6-31G** and 6-31+G** basis sets and assuming frequency scale factors identical to those used for the gas-phase calculations [36] – are also presented in Fig. 1. It is striking to see how much the spectra differ between calculations that include or exclude diffuse functions in the basis set. For the spectra in Fig. 1f and g, an attempt has been made to correlate the vibrational modes to those in Fig. 1a–c on the basis

Table 1
Experimental band positions (in cm^{-1}) in the gas-phase spectrum of deprotonated HBDI with proposed vibrational mode assignment (only dominant mode character is given).

Exp	Code[a]	Vibrational mode
1660	A	CO stretch imidazolinone
1558	C	Imidazolinone C=N stretching
1515	D	Asym vinyl C=C/phenoxide C—O stretch
~1455	E	CH_3 umbrella motions
1355		
1320		Various CH bending motions
1250		
1153	F	In-plane CH bending phenol ring
~1130		Delocalized in-plane CH bending
988		

[a] Letter codes correlate with bands labeled in Fig. 1.

of their mode character. However, many of the strong modes in the 1300–1550 cm^{-1} region in the 6-31+G** (PCM) spectrum have delocalized character and are not easily correlated to any of the modes labelled A through F. Although the vibrational mode characters of the 6-31G** (PCM) calculation are more straightforward to correlate with the gas-phase calculations, there is nevertheless not a clear one-to-one correlation with the experimental bands of Ref. [22]. We note that a Raman spectrum of the HBDI anion in aqueous solution, reported in Ref. [22] as well, was interpreted on the basis of Hartree–Fock calculations (HF/6-31+G*), for which inclusion of solvent effects using the PCM method sensitively improved the match with the experiment [23]. Nonetheless, the average absolute deviation for the main Raman bands was on the order of 40 cm^{-1}, while the deviation for the gas-phase bands listed in Table 1 is 15 cm^{-1}.

A closer inspection of the solution-phase spectrum of He et al. [22] in panel e of Fig. 1 reveals that it resembles to a significant extent the calculated gas-phase spectrum using the 6-31G** basis set (panel a), *i.e.*, the basis set not including diffuse functions. Even though the band positions are somewhat shifted, the overall intensity pattern of the bands in the 1450–1700 cm^{-1} range shows a remarkable similarity. One might be tempted to speculate whether restricting the wavefunctions by not including diffuse basis functions in the calculation correlates with the effect of the solvent restricting the electronic wavefunction in the experiment. Further study will be required to determine whether this apparent spectral similarity can indeed be explained by the influence of the solvent or whether it is purely coincidental.

3.2. IRMPD spectrum of the m/z 200 radical anion

Thermally induced dissociation of an even-electron ion, such as typically produced by ESI, commonly produces two even-electron fragments rather than two odd-electron fragments, as explained by Mandelbaum's "even-electron rule" [27]. Although various exceptions to this "rule" have been reported over the years [37], the present case is of interest to investigate further. Here, the closed-shell HBDI anion at *m/z* 215 dissociates by loss of 15 mass units, apparently producing two open-shell fragments, the unobservable neutral methyl radical and the anionic fragment observed at *m/z* 200. Loss of 15 mass units producing *m/z* 200 was also found to be the main dissociation pathway in collision- and laser-induced dissociation (CID, LID) of the HBDI anion [17]. Computations suggested that the methyl radical was lost from the imidazolinone nitrogen rather than from the carbon atom [17].

Here, we use IR spectroscopy to determine unambiguously the structure of the *m/z* 200 radical fragment of the HBDI anion, so that we can establish whether the methyl group is indeed lost from the imidazolinone nitrogen, but also whether radical site migration by hydrogen atom transfer occurs. To this end, we let deprotonated HBDI undergo CID in the front-end of the FTICR-MS by the

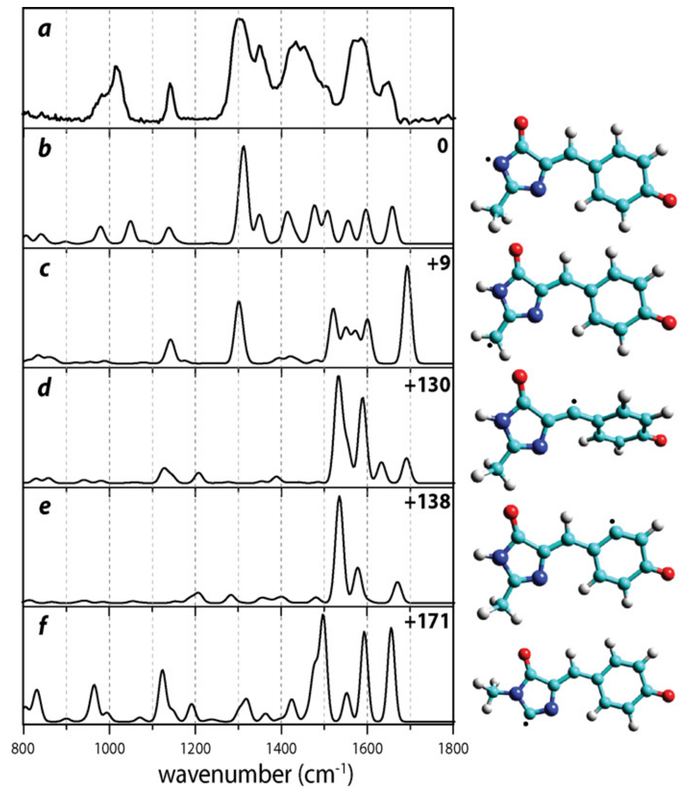

Fig. 2. Experimental spectrum of the main fragmentation product of the HBDI anion (a). The fragment is formed by loss of a neutral methyl group (CH_3) hence forming a radical anion at *m/z* 200. Panel (b) shows the calculated spectrum for the species formed by methyl loss from the imidazolinone nitrogen atom. Panels (c)–(e) show calculated spectra for its isomers formed by H-atom transfer (effectively moving the radical site). Panel (f) shows the calculated spectrum of the species formed by loss of the methyl group from the imidazolinone carbon atom. Relative free energies of the five isomers of the radical anion (B3LYP/6-31++G**) are given as well as their structures where the radical site is indicated.

application of a high cone voltage, which is optimized to maximize the production of the *m/z* 200 fragment anion. This fragment is then mass-isolated in the FT-ICR cell and its IRMPD spectrum is recorded. Upon IR multiple-photon excitation, the *m/z* 200 fragment is observed to photofragment mainly into mass channel *m/z* 131 with a minor contribution at *m/z* 199 due to loss of atomic hydrogen. Substantial electron detachment was also observed in this case, which is detected by leaking a low pressure of sulphur hexafluoride into the vacuum of the ICR cell; IR induced electron detachment is then detected by the appearance of a peak at *m/z* 146 [38]. To generate the experimental spectrum shown in Fig. 2a, dissociation and detachment signals were summed and the total yield was calculated.

HBDI possesses two methyl groups (see Scheme 1), one attached to one of the imidazolinone nitrogen atoms and one to one of the imidazolinone carbon atoms. Our calculations show that loss of the methyl group from the imidazolinone nitrogen atom leads to structures that are substantially lower in energy than the structures resulting from loss of a methyl group from the imidazolinone carbon atom. In addition, loss of a methyl group from either site may result in a radical anion with the radical at the respective imidazolinone nitrogen or carbon atom, or at any other site *via* radical site migration by H-atom transfer(s).

The IRMPD spectrum of the *m/z* 200 fragment of the HBDI anion is shown in the upper panel of Fig. 2. The spectrum is compared to the calculated spectrum of the radical anion where the methyl group on the imidazolinone nitrogen atom is removed (panel b), leaving an unpaired electron at this nitrogen atom. H-atom

Table 2
Experimental band positions (in cm^{-1}) for the m/z 200 radical anion fragmentation product of anionic HBDI, compared to band positions calculated for isomer b (see Fig. 2), for which the radical site is located on the imidazolinone nitrogen atom.

Exp		Calc	
Freq	Int[a]	Freq	Int[b]
1645	m	1649	253
1588	s	1588	232
1570	s	1547	158
1507	sh	1500	222
1453	s	1467	203
1428	s	1420	57
		1405	200
1350	s	1342	198
1303	vs	1307	559
		1296	196
1140	m	1132	108
1017	s	1043	154
981	w	974	115

[a] w, weak; m, medium; s, strong; vs, very strong; sh, shoulder.
[b] Integrated intensity in km/mol.

transfer can migrate the radical site onto the remaining methyl group (panel c), the vinylic carbon atom (panel d), or on one of the phenolic carbon atoms (panel e). The alternative dissociation reaction in which the methyl group is detached from the imidazolinone carbon atom leads to an isomer for which the calculated spectrum is shown in Fig. 2f. Our calculations indicate that the relative energy of this latter isomer is particularly high, and its H-atom transfer isomers are not shown in Fig. 2.

The experimental spectrum in Fig. 2a shows a rich and diagnostic vibrational pattern. From a comparison with the calculated spectra in Fig. 2b–f, one readily concludes that only the isomer with the radical site located on the imidazolinone nitrogen atom (panel b) matches with the experiment. The strong band observed in the experimental spectrum near 1300 cm^{-1} is predicted only for this isomer and for the isomer in which H-atom transfer has occurred from the remaining methyl group to the imidazolinone nitrogen atom (panel c). This isomer has a relatively low energy (+9 kJ/mol) and could thus be present as well on thermodynamic grounds. In that case a strong band would be expected near 1700 cm^{-1}, which is however not observed. We therefore conclude that isomer c is not present. All other isomers shown in Fig. 2 can easily be excluded on the basis of both their computed IR spectra as well as their relative energies. In contrast, an almost one-to-one match between the experimental and the theoretical spectrum is observed for the imidazolinone nitrogen radical (Fig. 2b), for which band positions are listed in Table 2. We thus conclude that in the dissociation process the methyl group is lost from the imidazolinone nitrogen atom and that no H-atom transfer occurs.

4. Conclusions

The gas-phase IR spectrum of a frequently employed mimic of the GFP chromophore, deprotonated HBDI (m/z 215), has been recorded by IRMPD spectroscopy using an FT-ICR mass spectrometer coupled to the FELIX beam line. Unlike the spectrum of the anion recorded in solution, the gas-phase experimental spectrum is convincingly reproduced by DFT calculations. Calculations show that good agreement with the experimental spectrum is obtained only if diffuse functions are included in the basis set.

IR photo-fragmentation as well as low-energy CID of the HBDI anion results mainly in a product anion at m/z 200, indicating the loss of a methyl radical forming a radical anion photoproduct. The structure of this odd-electron product has been investigated by recording its IRMPD spectrum, which suggests that the methyl group is lost from the imidazolinone nitrogen atom and that the radical site remains on that imidazolinone nitrogen atom.

Acknowledgments

We gratefully acknowledge the expert support by the FELIX staff, in particular of Drs. Britta Redlich and Alexander van der Meer. JO expresses special gratitude to the Stichting Physica for support. This study is part of the research program of FOM, which is financially supported by the Nederlandse Organisatie voor Wetenschappelijk Onderzoek (NWO).

References

[1] R.Y. Tsien, The green fluorescent protein, Annual Review of Biochemistry 67 (1998) 509–544.
[2] M. Ormo, A.B. Cubitt, K. Kallio, L.A. Gross, R.Y. Tsien, S.J. Remington, Crystal structure of the *Aequorea victoria* green fluorescent protein, Science 273 (1996) 1392–1395.
[3] C. Fang, R.R. Frontera, R. Tran, R.A. Mathies, Mapping GFP structure evolution during proton transfer with femtosecond Raman spectroscopy, Nature 462 (2009) 200–204.
[4] J.J. van Thor, Photoreactions and dynamics of the green fluorescent protein, Chemical Society Reviews 38 (2009) 3506.
[5] M. Chattoraj, B.A. King, G.U. Bublitz, S.G. Boxer, Ultra-fast excited state dynamics in green fluorescent protein: multiple states and proton transfer, Proceedings of the National Academy of Sciences of United States of America 93 (1996) 8362–8367.
[6] G. Palm, A. Zdanov, A. Wlodawer, The structural basis for spectral variations in green fluorescent protein, Nature Structural & Molecular Biology 4 (1997) 361–365.
[7] R.Y. Tsien, Constructing and exploiting the fluorescent protein paintbox (Nobel Lecture), Angewandte Chemie International Edition 48 (2009) 5612–5626.
[8] G.H. Patterson, J. Lippincott-Schwartz, A photoactivatable GFP for photolabeling of proteins and cells, Science 297 (2002) 1873–1877.
[9] A.R. Faro, P. Carpentier, G. Jonasson, G. Pompidor, D. Arcizet, I. Demachy, D. Bourgeois, Low-temperature chromophore isomerization reveals the photoswitching mechanism of the fluorescent protein Padron, Journal of the American Chemical Society 133 (2011) 16362–16365.
[10] T. Brakemann, A.C. Stiel, G. Weber, A.M.I. Testa, T. Grotjohann, M. Leutenegger, U. Plessmann, H. Urlaub, C. Eggeling, M.C. Wahl, S.W. Hell, S. Jakobs, A reversibly switchable GFP-like protein with fluorescence excitation decoupled from switching, Nature Biotechnology 29 (2011) 942–947.
[11] S.L. Maddalo, M. Zimmer, The role of the protein matrix in green fluorescent protein fluorescence, Photochemistry and Photobiology 82 (2006) 367–372.
[12] S.S. Stavrov, K.M. Solntsev, L.M. Tolbert, D. Huppert, Probing the decay coordinate of the green fluorescent protein: arrest of *cis–trans* isomerization by the protein significantly narrows the fluorescence spectra, Journal of the American Chemical Society 128 (2006) 1540–1546.
[13] M.W. Forbes, R.A. Jockusch, Deactivation pathways of an isolated green fluorescent protein model chromophore studied by electronic action spectroscopy, Journal of the American Chemical Society 131 (2009) 17038–17039.
[14] C.M. Megley, L.A. Dickson, S.L. Maddalo, G.J. Chandler, M. Zimmer, Photophysics and dihedral freedom of the chromophore in yellow, blue, and green fluorescent protein, Journal of Physical Chemistry B 113 (2009) 302–308.
[15] S.B. Nielsen, A. Lapierre, J.U. Andersen, U.V. Pedersen, S. Tomita, L.H. Andersen, Absorption spectrum of the green fluorescent protein chromophore anion in vacuo, Physical Review Letters 87 (2001) 228102.
[16] L.H. Andersen, A. Lapierre, S.B. Nielsen, I.B. Nielsen, S.U. Pedersen, U.V. Pedersen, S. Tomita, Chromophores of the green fluorescent protein studied in the gas phase, The European Physical Journal D 20 (2001) 597–600.
[17] L.H. Andersen, H. Bluhme, S. Boye, T.J.D. Jorgensen, H. Krogh, I.B. Nielsen, S.B. Nielsen, A. Svendsen, Experimental studies of the photophysics of gas-phase fluorescent protein chromophores, Physical Chemistry Chemical Physics 6 (2004) 2617–2627.
[18] M.W. Forbes, A.M. Nagy, R.J. Jockush, Photofragmentation of and electron photodetachment from a GFP model chromophore in a quadropole ion trap, International Journal of Mass Spectrometry 308 (2011) 155–166.
[19] D.A. Horke, J.R.R. Verlet, Photoelectron spectroscopy of the model GFP chromophore anion, Physical Chemistry Chemical Physics 14 (2012) 8511–8515.
[20] K. Lincke, T. Solling, L.H. Andersen, B. Klaerke, D.B. Rahbek, J. Rajput, C.B. Oehlenschlaeger, M.A. Petersen, M.B. Nielsen, On the absorption of the phenolate chromophore in the green fluorescent protein-role of individual interactions, Chemical Communications 46 (2009) 734–736.
[21] P. Schellenberg, E. Johnson, A.P. Esposito, P.J. Reid, W.W. Parson, Resonance Raman scattering by the green fluorescent protein and an analogue of its chromophore, The Journal of Physical Chemistry B 105 (2001) 5316–5322.
[22] X. He, A.F. Bell, P.J. Tonge, Isotopic labeling and normal-mode analysis of a green fluorescent protein chromophore, The Journal of Physical Chemistry B 106 (2002) 6056–6066.

[23] P. Altoe, F. Bernardi, M. Garavelli, G. Orlandi, F. Negri, Solvent effects on the vibrational activity and photodynamics of the green fluorescent protein chromophore: a quantum-chemical study, Journal of the American Chemical Society 127 (2005) 3952–3963.
[24] A.P. Esposito, P. Schellenberg, W.W. Parson, P.J. Reid, Vibrational spectroscopy and mode assignments for an analog of the green fluorescent protein chromophore, Journal of Molecular Structure 569 (2001) 25–41.
[25] A.G. Marshall, T.C.L. Wang, T.L. Ricca, Tailored excitation for Fourier Transform ion cyclotron resonance mass spectrometry, Journal of the American Chemical Society 107 (1985) 7893–7897.
[26] J.P. Merrick, D. Moran, L. Radom, An evaluation of vibrational frequency scale factors, The Journal of Physical Chemistry A 111 (2007) 11683–11700.
[27] M. Karni, A. Mandelbaum, The 'even-electron rule', Organic Mass Spectrometry 15 (1980) 53–64.
[28] G.W. Spitznagel, T. Clark, P. von Rague Schleyer, W.J. Hehre, An evaluation of the performance of diffuse function-augmented basis sets for second row elements, Na–Cl, Journal of Computational Chemistry 8 (1987) 1109–1116.
[29] R.A. Kendall, T.H. Dunning Jr., R.J. Harrison, Electron affinities of the first-row atoms revisited. Systematic basis sets and wave functions, Journal of Chemical Physics 96 (1992) 6796–6806.
[30] F. Jensen, Polarization consistent basis sets, III. The importance of diffuse functions, Journal of Chemical Physics 117 (2002) 9234–9240.
[31] B.J. Lynch, Y. Zhao, D.G. Truhlar, Effectiveness of diffuse basis functions for calculating relative energies by density functional theory, The Journal of Physical Chemistry A 107 (2003) 1384–1388.
[32] J. Oomens, J.D. Steill, Free carboxylate stretching modes, The Journal of Physical Chemistry A 112 (2008) 3281–3283.
[33] R.W. Williams, A.H. Lowrey, Effects of hydration on scale factors for ab initio force constants, Journal of Computational Chemistry 12 (1991) 761–777.
[34] R.C. Dunbar, D.T. Moore, J. Oomens, IR-spectroscopic characterization of acetophenone complexes with Fe^+, Co^+, and Ni^+ using free-electron-laser IRMPD, The Journal of Physical Chemistry A 110 (2006) 8316–8326.
[35] J. Oomens, B.G. Sartakov, G. Meijer, G. von Helden, Gas-phase infrared multiple photon dissociation spectroscopy of mass-selected molecular ions, International Journal of Mass Spectrometry 254 (2006) 1–19.
[36] A. Buczek, T. Kupka, S.P.A. Sauer, M.A. Broda, Estimating the carbonyl anharmonic vibrational frequency from affordable harmonic frequency calculations, Journal of Molecular Modeling 18 (2012) 2471–2478.
[37] R.D. Bowen, A.G. Harrison, Loss of methyl radical from some small immonium ions: unusual violation of the even-electron rule, Organic Mass Spectrometry 16 (1981) 180–182.
[38] J.D. Steill, J. Oomens, Action spectroscopy of gas-phase carboxylate anions by multiple photon IR electron detachment/attachment, The Journal of Physical Chemistry A 113 (2009) 4941–4946.